Dissimilatory bioreduction of iron(III) oxides by *Shewanella loihica* under marine sediment conditions

Robert Benaiges-Fernandez[1,2*], Jordi Palau[2,3], Francesco G. Offeddu[2], Jordi Cama[2], Jordi Urmeneta[1,4], Josep M. Soler[2] and Bernhard Dold[5,6]

[1]Department of Genetics, Microbiology and Statistics, Universitat de Barcelona, Barcelona, Catalonia, Spain

[2]Institute of Environmental Assessment and Water Research (IDAEA, CSIC), Barcelona, Catalonia, Spain

[3]Department of Mineralogy, Petrology and Applied Geology, Universitat de Barcelona, Barcelona, Catalonia, Spain

[4]Biodiversity Research Institute (IRBio), Universitat de Barcelona. Barcelona, Catalonia, Spain

[5]Department of Civil, Environmental and Natural Resources Engineering, Luleå University of Technology, Luleå, Sweden

[6]Sustainable Mining Research & Consultancy EIRL, San Pedro de la Paz, Chile

* Corresponding author

19

ABSTRACT

Shewanella is a genus of marine bacteria capable of dissimilatory iron reduction (DIR). In the context of deep-sea mining activities or submarine mine tailings disposal, dissimilatory iron reducing bacteria may play an important role in biogeochemical reactions concerning iron oxides placed on the sea bed. In this study, batch experiments were performed to evaluate the capacity of *Shewanella loihica* PV-4 to bioreduce different iron oxides (ferrihydrite, magnetite, goethite and hematite) under conditions similar to those in anaerobic sea sediments. Results showed that bioreduction of structural Fe(III) via oxidation of labile organic matter occurred in all these iron oxides. Based on the aqueous Fe (II) released, derived Fe(II)/acetate ratios and bioreduction coefficients seem to be only up to about 4% of the theoretical ones, considering the ideal stoichiometry of the reaction. A loss of aqueous Fe (II) was caused by adsorption and mineral transformation processes. Scanning electron microscope images showed that *Shewanella lohica* was attached to the Fe(III)-oxide surfaces during bioreduction. Our findings suggest that DIR of Fe(III) oxides from mine waste placed in marine environments could result in adverse ecological impacts such as liberation of trace metals in the environment.

38

39

40

41

42

43

44

45

1 INTRODUCTION

Iron is one of the most important elements on Earth due to its involvement in key biological processes, such as photosynthesis. However, the low solubility of Fe makes it not much bioavailable in most environments (Raiswell and Canfield, 2012). Iron is one of the controlling elements in many ecosystems, especially in marine environments (Field et al., 1998; Morel and Price, 2003). Some studies have shown that iron stimulates the growth of phytoplankton in high-nitrate, low-chlorophyll waters, which account for 25 % of the ocean (De Baar et al., 2005). Furthermore, iron participates in important biological processes such as atmospheric carbon dioxide consumption, dimethyl sulfide (DMS) production and organic matter (OM) degradation in sediments (Boyd and Ellwood, 2010). Bioavailability of iron in the sea also played a crucial role in the modulation of carbon dioxide concentration in the atmosphere in the geological past (Martin et al., 1990).

A marine sediment is an aphotic nutrient-rich and low-production zone where most microorganisms are heterotrophic (Fenchel, 1969). In anoxic reduced zones of the sediment, there are OM-degrading anaerobic microorganisms that use inorganic compounds other than oxygen as terminal electron acceptors (TEAs) for the electron transport respiratory chain (Lovley, 1991). Dissimilatory iron reduction mediated by microorganisms uses Fe(III) as TEA to produce Fe(II) species. This process is coupled to the degradation of simple OM and is carried out by different genera of bacteria, like *Geobacter* or *Shewanella (Lovley and Phillips, 1986)*. In marine sediments, metabolic products of degradation serve as electron donors for the terminal oxidizing bacteria, which use inorganic TEAs for a complete oxidation of organic matter. Moreover, iron reduction besides sulfate reductors are the most important terminal oxidation processes in the upper anoxic zone (Thamdrup, 2000). For instance, in artic marine sediments lactate (among acetate, propionate and isobutyrate) is degraded in the marine sediment by iron and sulfate reducers (Finke et al., 2007).

The *Shewanella* genus is well known for itspresence in marine sediments and for its metabolic capacity (Hau and Gralnick, 2007). *Shewanella* can use oxygen, nitrate and heavy metals as TEAs. Some strains may even degrade recalcitrant organic compounds, such as chlorinated solvents, providing the genus with the potential to be applied in bioremediation studies (Roh et al., 2006). *Shewanella loihica* is a species from the genus Shewanella isolated from a submarine volcano in Loihi, Hawaii (Gao et al., 2006). The metabolic versatility and ubiquitous presence in the marine environment make *Shewanella loihica* a suitable candidate for bioreduction studies. Earlier studies on the capacity and mechanisms of *Shewanella* to bioreduce ferric iron in fresh water have shown that (i) it is able to reduce not only soluble Fe

(III) compounds but also (Fe) (III)-bearing minerals such as magnetite (Fe_3O_4) through polysaccharide attachment (Dong et al., 2000) and that (ii) biotic iron reduction coupled to OM degradation requires a direct contact between the microorganisms and the poorly soluble mineral surface (Tugel et al., 1986). However, bioreduction of magnetite and other iron oxides and hydroxides (ferrihydrite, goethite and hematite) under marine conditions has not yet been studied.

The fate of iron oxides in seafloor sediments has a major interest for potential sea water contamination caused by deep-sea mining activities or marine disposal of mine tailings, which were practices widely spread worldwide (Ellis and Ellis, 1994) although currently banned in most of the countries (Dold, 2014). For instance, marine contamination associated with continuous tailings disposal has been reported in. Chañaral Bay in northern coast of Chile (Dold, 2006; Medina et al., 2005) and Portman Bay in the south-east coast of Spain (Manteca et al., 2014). In mine tailings originated from sulfide-rich ores the contained Fe(III)-oxides incorporate Mn, Al, Cr, Co, Ni, Zn, V, Pb and As (Knipping et al., 2015; Nadoll et al., 2014). Valence II and III metal cations can be absorbed on the iron oxides or isomorphously substitute iron in the crystalline oxide structure (Cornell and Schwertmann, 1996). Offshore disposal of these mine tailings may result in adverse ecological impacts as bioreductive dissolution of Fe(III) oxides releases aqueous Fe(II) together with trace metals and metalloids co-precipitated or structurally incorporated in Fe (III) oxides (Zachara et al., 2001). Thus, an undesired bioaccumulation of metals and metalloids in sea sediments, in secondary plumes and in the water column and an increase in trophic transfer of metals could occur (Morello et al., 2016; Ramirez-Llodra et al., 2015). A better understanding of the interaction between Fe(III) oxides and microorganisms capable to bioreduce Fe(III) sheds new light on the bioavailability of iron in the ocean and on potential environmental consequences of sea mining activities and marine disposal of mine tailings.

To this end, Fe(III) oxides (synthetic ferrihydrite, commercial goethite, magnetite and hematite and field specimens with different contents of iron oxides and other minerals) were reacted in the laboratory in the presence of *Shewanella loihica* strain PV-4, whose ecophysiology makes it optimal for Fe(III)-bioreduction under marine sediment conditions. Two different experiments were performed to elucidate the kinetics of Fe(III) bioreduction and to examine the bacteria-mineral surface interaction.

2   MATERIALS AND METHODS

2.1   Sample characterization

The iron oxide samples used in this study have three different sources: three samples were commercial powders of magnetite, hematite and goethite purchased from Sigma Aldrich; one sample of 2L ferrihydrite was synthesized in the laboratory following the procedure described by Cornel and Shwertmann (1991); and three samples were field specimens with different contents of magnetite (V1 from Distrito Algarrobo, Chile, TB from Lago Sur, Chile, and M1 from Malmberget, Sweden). Sample V1 also contained hematite. Powder X-ray diffraction (XRD) analysis and Rietveld refinement (Young, 1995), using a Bruker D8 A25 Advance X-ray diffractometer θ- θ with CuKα1 radiation, showed that the commercial and synthesized samples were composed of the respective iron oxides and no accessory minerals were identified. Rietveld analysis confirmed that no impurities were present in the samples. As for the field samples, magnetite was present in all of them (ranging from 19 to 89 wt. % for V1 and M1, respectively), hematite was only present in V1 (40 wt. %) and goethite was not detected (Table 1). Other minerals identified were silicates (hornblende, and Fe-actinolite) and phosphates (hydroxyapatite) (Table 1).

The size fraction of the commercial powders was about 5 μm. Synthesized 2L ferrihydrite was ground using an agate mortar and pestle and sieved to a size fraction of 5 - 60 μm. Fragments of field samples were similarly ground and sieved to a size fraction of 60 - 100 μm. These powdered samples were used in batch experiments to study the Fe(III) bioreduction reaction. The specific surface area of all these samples was determined by the Brunauer-Emmett-Teller (BET) method (Brunauer et al., 1938) using a Gemini 2370 surface area analyzer and 5-point N_2 adsorption isotherms. Sample degassing with nitrogen lasted for 2 h at 137 °C. Data uncertainty was around 10 %. Synthesized ferrihydrite showed the largest value (181 m^2 g^{-1}) and M1 and TB the lowest ones (0.6 and 0.2 $m^2 g^{-1}$, respectively; Table 2).

2.2   Bacterial culture

Shewanella loihica strain PV-4 was obtained from the German Collection of Microorganisms and Cell Cultures (DSMZ 17748). To obtain a bacterial suspension for the starting inoculum, cells were cultivated in M1 medium (Gao et al., 2006) supplemented with 10 mM of sodium lactate as electron donor and carbon source and 10 mM of Fe(III) citrate as electron acceptor. Cultures were incubated anaerobically for 24 h at 30 °C and then harvested by centrifugation (5000 rpm for 10 min). The pellet was re-suspended in synthetic seawater

143 prepared previously following the standard protocol D1141-98 (ATSM International).

144 Centrifugation and pellet resuspension were repeated three times as a washing step.

145   A medium simulating seawater (hereafter referred to as marine medium) was

146 developed for the experiments. A basal medium of synthetic seawater (ASTM D1141-98) was

147 amended with sodium lactate (10 mM) as an electron donor and carbon source, ammonium

148 chloride (1.87 mM) as a source of nitrogen, and TRIS-HCl (10 mM) as a pH-buffer. The pH of

149 the medium was adjusted to 8.2 with 0.1 N NaOH solution. The final medium was sterilized by

150 autoclave (121 °C for 20 min).

2.3   Batch experiments with powdered samples

152   In all batch experiments, 0.25 ± 0.01 g of powdered sample were placed in 25 mL glass

153 vials capped with Teflon plugs and then sterilized by autoclave (121 °C for 20 min). Previous

154 studies (Das et al., 2010; Mazzetti and Thistlethwaite, 2002) showed a thermal transformation

155 of ferrihydrite to hematite could occur. A test performed with ferrihydrite showed that XRD

156 analyses after the sterilization revealed no mineral changes in this stage.

157   The vials were filled with 25 mL of marine medium, keeping a 1% solid/liquid ratio

158 (g/mL), and inoculated with *Shewanella loihica* to an approximate final number of $1 \cdot 10^{7}$

159 colony-forming units (cfu) mL^{-1}, measured by agar culture (LB). The vials were sealed with

160 screw caps, leaving a minimal head space (small air bubble) to prevent overpressure, and

161 statically immersed in a thermostatic water bath at 10 ± 1 °C in the dark. These conditions with

162 the use of the marine medium mimicked the suboxic zone in marine sediments (Jørgensen and

163 Kasten, 2006; Rosselló-Mora et al., 1999). Abiotic controls without inoculum of *Shewanella*

164 *loihica* were also prepared under the same conditions as biotic experiments.

165   For each solid sample, a single-point batch experiment was carried out. Five vials were

166 prepared as replicates, and each one was sacrificed at different time spans (13, 27, 47, 70 and

167 111 days). Sampling was performed in a glove box with N_2 atmosphere to maintain the anoxic

168 conditions. The vials were shaken just before sampling and then the medium from the vial was

169 totally recovered, sampled and filtered using a sterile syringe and syringe filters (0.22 μm pore

170 size). Sample aliquots were used for pH/Eh measurements and for chemical analyses of cations

171 and anions. To evaluate the carbon and energy source consumption, lactate and acetate, being

172 the latter the oxidation end product under anaerobic conditions, were measured. For ion

173 analysis a volume of 10 mL was preserved at pH < 2 by adding 100 μL of 60 % (v/v) HNO_3

174 solution. For Fe(II)/Fe(III) measurements by Phenanthroline colorimetry (Stucki, 1981), an

175 additional volume of 10 mL was preserved with the addition of 100 μL of 6 M HCl solution.

176 Thereafter, all samples were stored at 4 °C in the dark until analysis.

177   2.3.1   Chemical analyses

178   Measurements of pH (± 0.02 pH units) and Eh (± 10 mV) were performed in the glove

179 box using pH and Eh electrodes (Crison and SenTix ORP, Ag/AgCl, WTW, respectively).

180 Oxidation-reduction potential readings were converted to standard Eh values by correcting for

181 the electrode potential of the reference hydrogen electrode. Total iron was analyzed by

182 Inductively Coupled Plasma Mass Spectrometry (ICP-MS, Perkin- Elmer 3000). Owing to the

183 high dissolved iron concentrations in the experiments with ferrihydrite, iron measurements

184 were performed using ICP–Optical Emission Spectroscopy (ICP-OES). The uncertainty of the

185 ICP-MS (and ICP-OES) measurements was better than ± 5 %. Total iron measured was checked

186 to be Fe (II) with a modified protocol of the Phenanthroline method (Stucki, 1981). Lactate and

187 acetate concentrations were determined by high performance liquid chromatography (HPLC).

188 The equipment used consisted of a Waters 600 HPLC pump controller equipped with an

189 Aminex HPX-87H column (300 x 7.8 mm), BioRad, and a Waters 717 plus autoinjector.

190 Triplicates were performed for iron, lactate and acetate measurements.

191   **2.4   Fe (II)-ferrihydrite adsorption experiments**

192 Fe(II) adsorption on powdered ferrihydrite in marine medium (0.5 g of ferrihydrite and 50 mL

193 of solution, 1% w/v) was determined in gently mixed batch experiments at room temperature

194 (23 ± 2 °C). Different amounts of $FeCl_2$ were added to distinct vials, from 0.4 to 40 mM, in

195 order to get a wide range of initial Fe(II) aqueous concentration in the experiment. Samples

196 were collected after reaching equilibrium at 24 h (Dzombak and Morel, 1990) to measure total

197 and ferrous iron by the phenanthroline method. At the end of the experiments the solid

198 fractions were retrieved, freeze dried and preserved under nitrogen atmosphere until analysis.

199 Subsequently, XRD-Rietveld analyses and measurement of BET specific surface areas were

200 performed. The concentration of adsorbed Fe(II) was determined by subtracting the aqueous

201 ferrous iron concentration after equilibration from the initial concentration according to (1):

202 $$C_{Fe-ads} = (C_{Fe-i} - C_{Fe-eq}) \cdot \frac{V}{M} \qquad\qquad (1)$$

203 where C_{Fe-ads} is the amount of adsorbed iron per gram of ferrihydrite, C_{Fe-i} and C_{Fe-eq} are the

204 initial and equilibrium aqueous concentrations of Fe(II), respectively, V is the volume of

205 solution and M is the mass of ferrihydrite.

206

2.5   Experiments with microbial cells and field samples

208   Surface mineral-bacteria interaction was investigated by scanning electron microscope

209   (SEM). Fragments of field samples (M1 and TB) were cut down to small rectangular pieces

210   (surface of $\approx$ 10 mm^2 and $\approx$ 3 mm thick) in order to fit into sample holders used for the critical

211   point drying technique. These pieces were used to study the interaction between *Shewanella*

212   and the surface of the iron oxides. Top surfaces were polished by conventional metallographic

213   polishing to improve the observation of the surface mineral-bacteria interaction by SEM. The

214   M1 and TB pieces were placed in 200 mL bottles filled with marine medium (synthetic sea

215   water) without head space and incubated with $1 \cdot 10^7$ cfu mL^{-1} of *Shewanella loihica.*

216   Experiments were conducted in the N$_2$-atmosphere glove box in the dark for 115 days at 25 ^{o}C.

217   At the end of the experiments, the pieces incubated with *Shewanella* were retrieved and

218   treated for 2 h with a glutaraldehyde 2.5 % w/v in 0.1 M phosphate buffered saline (PBS) cell-

219   fixation solution. Several washes with PBS (10 min each) were done, and post-fixation of the

220   mineral pieces was carried out using 1 % osmium tetraoxide and 0.8 % potassium ferricyanide

221   in 0.1 M PBS for up to 2 h in darkness. To evaluate potential effects of the dehydration process

222   on the bacteria structure, two different dehydration methods were carried out. In one

223   dehydration method the critical point drying technique was performed by replacing water in

224   the samples with increasing concentrations of ethanol (50-100 %) (Anderson, 1951). In the

225   other method sample dehydration was performed using a hexamethyldisilazane (HMDS)

226   solution (Nation, 1983). Thereafter, all samples were coated with carbon before SEM

227   observation (Hitachi H-4100FE instrument under a 15–20 kV potential in a high vacuum) using

228   the backscattered electron detector (BSD) in Field Emission (FE) and an energy-dispersive

229   spectrometer (EDS).

3   RESULTS

3.1   Bioreductive dissolution of Fe-oxides

232   Dissolution of the iron oxide minerals and production of aqueous Fe(II) did not take

233   place in the abiotic control experiments. In contrast, bioreductive dissolution occurred in all

234   experiments inoculated by *Shewanella loihica*. Figure 1 shows the variation of total aqueous

235   iron concentration over time for the experiments with synthetic and commercial samples.

236   Measured total aqueous iron in all the experiments was confirmed to be Fe (II) by the

237   phenanthroline method. Aqueous iron concentration increased over time in the experiment

238   with hematite (Fig. 1a), initially increased and then decreased in the case of goethite (Fig. 1b)

239   and increased and levelled off in the experiments with magnetite and ferrihydrite (Fig. 1c,d).

240   The highest Fe(II) concentration (1.3 mM) was reached in the ferrihydrite experiment. In all

241   experiments, the change in aqueous ferrous iron concentration was accompanied by

242   consumption of lactate and production of acetate. Only in the case of ferrihydrite experiment

243   lactate was totally consumed. For the experiments prepared with field samples, reductive

244   dissolution of the iron oxides showed similar trends (Fig. 2), in which iron increased in different

245   steps (Fig. 2a,c) or gradually (Fig. 2b). The concentrations of released iron were lower than

246   those of the synthetic and commercial samples (< 0.03 mM). As observed for the experiments

247   with synthetic and commercial samples, consumption of lactate and production of acetate

248   accompanied the ferrous iron release.

249   The measured ferrous iron and acetate concentrations throughout the experiments

250   were used to estimate initial bioreduction coefficients based on the initial release of iron and

251   acetate associated with the microbial activity. These coefficients were calculated by linear

252   regression of the first two sampling points for ferrihydrite and the first three ones for the other

253   oxide experiments using the following expressions (2,3):

254 $$k_{biored-Fe} \ = \ \frac{C_{Fe(II)} \cdot V}{\Delta t \cdot M} \qquad (2)$$

255

256 $$k_{biored-Ac} \ = \ \frac{C_{acetate} \cdot V}{\Delta t \cdot M} \qquad (3)$$

257   where $C_{Fe(II)}$ and $C_{acetate}$ are the measured iron and acetate concentrations (μM), V is the

258   solution volume (L), M is the Fe(III)-oxide mass (g) and t is time (d). Linear regressions showed

259   R^2 values between 0.8 and 0.99. The values of the iron and acetate bioreduction coefficients

260   are listed in Table 2. Figure 3a shows that the bioreduction coefficient ($\mu mol \ g_{oxide}^{-1} \ d^{-1}$) for the

261   ferrihydrite experiment is much larger than those of the other samples. However, when the

262   coefficients are normalized with the specific BET surface area ($\mu mol \ m^{-2} \ d^{-1}$) the coefficients of

263   magnetite are higher (Fig. 3b).

264   In all experiments, pH slightly decreased from 8.2 to an average pH of 7.8 (Fig. S1)

265   whereas Eh significantly decreased from 300 mV to an average value of 18.5 mV (Fig. S1).

266 ## 3.2   Fe(II)-ferrihydrite adsorption

267   Due to the high specific surface area of ferrihydrite (181 m^2 g^{-1}) compared to the other
268 iron oxides investigated (Table 1), this phase was used to evaluate Fe(II) adsorption on Fe(III)-
269 oxides in the marine medium. Figure 4 shows the measured adsorption of Fe(II) on powdered
270 ferrihydrite. The amount of adsorbed Fe (II) increased with Fe (II) aqueous concentration,
271 exceeding the theoretical adsorption capacity of ferryhydrite (0.6 mmol g^{-1}) (Hiemstra, 2013).
272 The XRD patterns and Rietveld semi-quantitave analysis of the retrieved ferrihydrite allowed us
273 to elucidate the mineralogical change at the end of the experiment and showed the presence
274 of both ferrihydrite (≈10 wt%) and magnetite (≈ 90 wt%) (Fig. 5).

275 ## 3.3   Bacteria and Fe-oxide surfaces

276   Independently of the dehydration technique used to preserve the bacteria structure,
277 SEM images of the reacted field samples showed the presence of bacteria (*S. loihica*) attached
278 on the iron-oxide surfaces (Fig. 6). Bacteria cells colonized the iron-oxide surfaces, either as
279 individual cells or forming clusters. Most of the cells were attached preferably on the iron-
280 oxide surfaces rather than on the surfaces of the other minerals present in the field samples
281 (Fig. 6a). Extracellular structures by *S. loihica* have been observed suggesting that bacteria
282 connect with the mineral surface and with other cells (Fig. 6b,c).

283 # 4   DISCUSSION

284 ## 4.1   Aqueous chemistry

285   The capacity of *Shewanella* to reduce soluble (e.g. iron citrate) or structural (e.g.
286 biogenic magnetite) ferric iron has been studied (Kostka and Nealson, 1995), but its capacity to
287 reduce magnetite and other iron-oxide minerals under marine conditions remained unknown.
288 Our study demonstrates that *S. loihica* was able to bioreduce not only magnetite, but also
289 hematite, goethite and ferrihydrite in conditions similar to those found in anoxic marine
290 environments, such as in seafloor sediments and in offshore mine-tailings disposal sites
291 (Ramirez-Llodra et al., 2015). It appeared that *S. loihica* used the structural ferric iron of the
292 iron oxides as an electron acceptor in the respiratory chain (Tugel et al., 1986). In the
293 experiments, a simultaneous consumption of light organic matter (lactate) to produce acetate
294 was observed along with an increase in aqueous Fe(II). Production of acetate was attributed to
295 the anaerobic metabolism of the bacteria during ferric iron reduction. This finding is in

296   agreement with previous studies showing that the metabolism of *S. loihica* was sustained by

297   the production of acetate from lactate, which acts as electron donor (Scott and Nealson, 1994;

298   Tang et al., 2007).

299   Bioreduction may be expressed in a simple form as (Lovley, 1991) (4):

300      $Lactate^- + 4Fe^{3+} + 2H_2O \rightarrow acetate^- + HCO_3^- + 4Fe^{2+} + 5H^+$ (4)
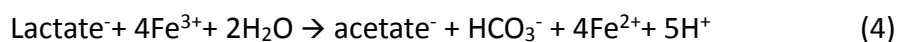
301   where one and four moles of acetate and ferrous iron are respectively produced (i.e.,

302   Fe(II)/acetate ratio = 4). Experiments with high lactate consumption and acetate formation

303   correlated well with those having high aqueous ferrous iron concentration. In the ferrihydrite

304   experiment, however, bioreduction was halted by total exhaustion of lactate (Fig. 1d). Mass

305   balance between lactate consumption and acetate production showed carbon deficit in all

306   experiments (lactate consumed > acetate produced). In a first stage (≈ <12h) of bioreduction

307   experiments, *Shewanella loihica* consumed all the remaining oxygen in solution in the full

308   oxidation of lactate to CO_2 via the aerobic metabolic pathway. The observed carbon mismatch

309   (reaching up to ≈20 %) was attributed to both carbon assimilation in biomass formation during

310   microbial growth and the use of the aerobic metabolic pathway in oxygen consumption by

311   *Shewanella loihica*.

312   According to the bioreduction reaction (Eq. 4), a significant deficit of ferrous iron, based on

313   measured aqueous Fe(II) relative to acetate, was found in all experiments. The Fe(II)/acetate

314   ratios range between 0.03 and 0.17, which is between 0.7 % and 4.3% of the stoichiometric

315   ratio (Table 2). Several previous studies (Benner et al., 2002; Bonneville et al., 2004; Roden et

316   al., 2000) reported a similar Fe(II) deficit, suggesting that (1) the apparent extent of

317   bioreduction based on measured aqueous Fe(II) reached only about 3% solubilization of initial

318   Fe(III) and (2) Fe(III) reduction could then be largely underestimated due to adsorption of Fe(II)

319   on the dissolving iron oxides and/or formation of secondary mineral phases containing

320   structural Fe(II).

321   In the current study, the measurement of adsorption of Fe(II) on powdered ferryhidrite

322   in marine medium (Fig. 4) indicated a probable adsorption of solubilized ferrous iron, as it has

323   also been found for other Fe(III)-oxides in previous studies using aqueous solutions with a

324   composition different than in our study (Larese-Casanova and Scherer, 2007; Rajput et al.,

325   2016). Considering the adsorption capacity of ferryhidrite (0.6 mmol g^{-1}) and the released

326   acetate in the ferrihydrite bioreduction experiment (Fig. 1d), a Fe(II)/acetate ratio of 3.25

327   would be obtained if only adsorption of ferrous iron had occurred. Therefore, the marked Fe

328   deficit observed (Fe(II)/acetate = 0.17; Table 2) cannot be explained by adsorption of ferrous

329   iron alone. Moreover, the Fe(II)-ferrihydrite adsorption experiments showed that the adsorbed

330   Fe(II) exceeded the maximum capacity (0.6 mmol g^{-1}; Fig. 4). This indicated that an additional

331   process, such as ferrihydrite transformation to magnetite, could be responsible for the extra

332   Fe(II) uptake. A comparison between the XRD patterns of non-reacted and reacted ferrihydrite

333   samples showed the presence of magnetite, a more crystalline phase (Fig. 5), confirming the

334   occurrence of magnetite formation. Previous studies suggested that the Fe(III)-oxide-

335   magnetite transformation is driven by an electron transfer between the absorbed Fe(II) and

336   Fe(III) in iron oxides, resulting in the formation of nano-crystalline, stoichiometric magnetite

337   (Byrne et al., 2011; Williams and Scherer, 2004). This mineralogical transformation may be

338   expressed as (5):

339     $$2Fe(OH)_3 + Fe^{2+} \longleftrightarrow Fe_3O_4 + 2H_2O + 2H^+ \qquad (5).$$
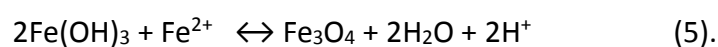
340   It is suggested that in alkaline environments magnetite is the most stable iron oxide

341   phase (Tronc et al., 1992), in contrast to lepidocrocite and goethite in neutral environments

342   (Boland et al., 2014). Simultaneous Fe(II) adsorption and mineral transformation could

343   therefore explain the systematically high deficit of aqueous ferrous iron. These two processes,

344   which act as a sink for dissolved biogenic ferrous iron, were also observed in *Geobacter*

345   mediated ferrihydrite bioreduction (Chen et al., 2018).

346   The estimated initial bioreduction coefficients differed between the different oxides

347   studied (Table 2). Bioreduction kinetics is dependent on the reactive surface area of the iron

348   oxides, which plays a key role in the process (Burdige et al., 1992). Ferrihydrite has the largest

349   surface area (Table 1), up to three orders of magnitude higher than that of the other minerals.

350   As a result, the bioreduction coefficient of ferrihydrite shows the highest value (5.49 µmol of

351   Fe(II) g$_{oxide}$$^{-1}$ d^{-1};Fig. 3a). In contrast, the lowest bioreduction coefficient corresponds to

352   goethite(Table 2), commercial powder (0.026 µmol of Fe(II) g$_{oxide}$$^{-1}$ d^{-1}; Fig. 3a). Nevertheless,

353   when microbial bioreduction coefficients were normalized with the specific surface area of the

354   oxides, magnetite, either synthetic or natural (Magnetite and M1) shows the highest

355   bioreduction coefficient (0.034 µmol Fe(II) m^{-2} d^{-1} for Magnetite and 0.309 µmol Fe(II) m^{-2} d^{-1}

356   for for M1; Fig. 3b). According to the normalized acetate coefficients, both commercial and

357   field magnetite samples showed the highest acetate production compared to other

358   commercial and synthetic samples (0.249 µmol acetate m^{-2} d^{-1} and 5.31 µmol acetate m^{-2} d^{-1},

359   respectively). These phases therefore show high preference for *Shewanella*'s bioreduction.

360   Yet, the high values of the magnetite bioreduction coefficient could be also associated with an

361   extra release of ferrous iron from the lattice of the magnetite (Kostka and Nealson, 1995).

362   Furthermore, if Fe(III) of the magnetite lattice is reduced to Fe(II), an increase in crystal radius

363 (with IV coordination) from 63 to 77 pm might destabilize magnetite structure, yielding high

364 coefficient values (Shannon, 1976). The variability in the bioreduction coefficients of the

365 studied iron oxides could be attributed to the differences in the intrinsic mineral properties,

366 such as the degree of crystallinity, grain size and impurity content (Li et al., 2012; O'Loughlin et

367 al., 2010).

4.2 *Shewanella loihica* and Fe-oxide surfaces

369 Bacteria use several strategies to perform bioreduction process. A well-known strategy

370 is the contact of bacteria with mineral surfaces, allowing the electron transport (Burdige et al.,

371 1992). SEM images showed *Shewanella loihica* cells colonizing the iron-oxide surfaces (Fig. 6a),

372 either as individual cells or forming clusters. In addition, the SEM images revealed the

373 presence of extracellular structures apparently connecting single cells with the mineral surface

374 and/or with other cells (Fig. 6b,c). In fact, previous studies have shown that the genera

375 *Shewanella* is able to develop extracellular structures to perform the electron exchange in the

376 bioreduction process (i.e. nanowires) (Gorby et al., 2006; Pirbadian et al., 2014; Shi et al.,

377 2016). A similar morphology between the extracellular structures in our study and those

378 reported in previous studies exist. Nevertheless, to fully prove the electron-exchange capacity

379 of the extracellular structures observed in this work, further studies are necessary.

5 CONCLUSIONS

381 *Shewanella loihica* is able to dissolve Fe (III) oxides via dissimilatory iron reduction

382 under conditions of anoxic marine sediments. The deficit of aqueous ferrous iron relative to

383 acetate produced during bioreduction was explained by adsorption of Fe(II) on the dissolving

384 iron oxides and transformation of the iron oxides into stoichiometric magnetite. Hence,

385 calculated bioreduction coefficients based on measured aqueous Fe(II) account for only up to

386 about 4% of the actual reaction, considering the theoretical release of Fe (II) and acetate

387 productions. During bioreduction, *Shewanella loihica* colonizes the surface of the iron oxides.

388 Results indicate a potential unfavorable role of iron-oxide bioreduction in deep-sea

389 mining activities or coastal mine-tailings disposal, where release of trace and toxic metals

390 represents an environmental threat. Furthermore, the iron released from metal mine tailings

391 disposed offshore could affect primary production, jeopardizing the resilience of offshore

392 ecosystems. However, a positive implication of iron-oxide bioreduction is found for

393   biotechnology as iron-oxide bioleaching could potentially be used for recovery of iron and
394   trace elements in metallurgical treatments.

395   **Acknowledgements**

403

6   References

Anderson, T.F., 1951. TECHNIQUES FOR THE PRESERVAATION OF THREE‑DIMENSIONAL STRUCTURE IN PREPARING SPECIMENS FOR THE ELECTRON MICROSCOPE. Transactions of the New York Academy of Sciences 13, 130-134.

Benner, S.G., Hansel, C.M., Wielinga, B.W., Barber, T.M., Fendorf, S., 2002. Reductive dissolution and biomineralization of iron hydroxide under dynamic flow conditions. Environmental Science & Technology 36, 1705-1711.

Boland, D.D., Collins, R.N., Miller, C.J., Glover, C.J., Waite, T.D., 2014. Effect of solution and solid-phase conditions on the Fe (II)-accelerated transformation of ferrihydrite to lepidocrocite and goethite. Environmental science & technology 48, 5477-5485.

Bonneville, S., Van Cappellen, P., Behrends, T., 2004. Microbial reduction of iron (III) oxyhydroxides: effects of mineral solubility and availability. Chemical Geology 212, 255-268.

Boyd, P., Ellwood, M., 2010. The biogeochemical cycle of iron in the ocean. Nature Geoscience 3, 675.

Brunauer, S., Emmett, P.H., Teller, E., 1938. Adsorption of gases in multimolecular layers. Journal of the American chemical society 60, 309-319.

Burdige, D.J., Dhakar, S.P., Nealson, K.H., 1992. Effects of manganese oxide mineralogy on microbial and chemical manganese reduction. Geomicrobiology Journal 10, 27-48.

Byrne, J., Telling, N., Coker, V., Pattrick, R., Van Der Laan, G., Arenholz, E., Tuna, F., Lloyd, J., 2011. Control of nanoparticle size, reactivity and magnetic properties during the bioproduction of magnetite by Geobacter sulfurreducens. Nanotechnology 22, 455709.

Chen, Z., Zhang, Y., Luo, Q., Wang, L., Liu, S., Peng, Y., Wang, H., Shen, L., Li, Q., Wang, Y., 2018. Maghemite (γ-Fe2O3) nanoparticles enhance dissimilatory ferrihydrite reduction by Geobacter sulfurreducens: Impacts on iron mineralogical change and bacterial interactions. Journal of Environmental Sciences.

Cornel, R., Shwertmann, U., 1991. Iron oxides in the laboratory. Preparation and characterization. VCH Editions, Weinhein, Germany.

Cornell, R., Schwertmann, U., 1996. The Iron Oxides: Structures, Properties, Reactions, Occurrences and Uses. VCH Verlagsgesellshaft GMBH, Weinheim, Germany, 533-559.

Das, S., Hendry, M.J., Essilfie-Dughan, J., 2010. Transformation of two-line ferrihydrite to goethite and hematite as a function of pH and temperature. Environmental science & technology 45, 268-275.

De Baar, H.J., Boyd, P.W., Coale, K.H., Landry, M.R., Tsuda, A., Assmy, P., Bakker, D.C., Bozec, Y., Barber, R.T., Brzezinski, M.A., 2005. Synthesis of iron fertilization experiments: from the iron age in the age of enlightenment. Journal of Geophysical Research: Oceans 110.

Dold, B., 2006. Element flows associated with marine shore mine tailings deposits. Environmental science & technology 40, 752-758.

Dold, B., 2014. Submarine tailings disposal (STD)—A review. Minerals 4, 642-666.

Dong, H., Fredrickson, J.K., Kennedy, D.W., Zachara, J.M., Kukkadapu, R.K., Onstott, T.C., 2000. Mineral transformations associated with the microbial reduction of magnetite. Chemical Geology 169, 299-318.

Dzombak, D.A., Morel, F., 1990. Surface complexation modeling: hydrous ferric oxide. John Wiley & Sons.

Ellis, D., Ellis, K., 1994. Very deep STD. Marine Pollution Bulletin 28, 472-476.

Fenchel, T., 1969. The ecology of marine microbenthos IV. Structure and function of the benthic ecosystem, its chemical and physical factors and the microfauna commuities with special reference to the ciliated protozoa. Ophelia 6, 1-182.

Field, C.B., Behrenfeld, M.J., Randerson, J.T., Falkowski, P., 1998. Primary production of the biosphere: integrating terrestrial and oceanic components. science 281, 237-240.

453   Finke, N., Vandieken, V., Jørgensen, B.B., 2007. Acetate, lactate, propionate, and isobutyrate as
454   electron donors for iron and sulfate reduction in Arctic marine sediments, Svalbard. FEMS
455   Microbiology Ecology 59, 10-22.
456   Gao, H., Obraztova, A., Stewart, N., Popa, R., Fredrickson, J.K., Tiedje, J.M., Nealson, K.H., Zhou,
457   J., 2006. Shewanella loihica sp. nov., isolated from iron-rich microbial mats in the Pacific
458   Ocean. International Journal of Systematic and Evolutionary Microbiology 56, 1911-1916.
459   Gorby, Y.A., Yanina, S., McLean, J.S., Rosso, K.M., Moyles, D., Dohnalkova, A., Beveridge, T.J.,
460   Chang, I.S., Kim, B.H., Kim, K.S., 2006. Electrically conductive bacterial nanowires produced by
461   Shewanella oneidensis strain MR-1 and other microorganisms. Proceedings of the National
462   Academy of Sciences 103, 11358-11363.
463   Hau, H.H., Gralnick, J.A., 2007. Ecology and biotechnology of the genus Shewanella. Annu. Rev.
464   Microbiol. 61, 237-258.
465   Hiemstra, T., 2013. Surface and mineral structure of ferrihydrite. Geochimica et Cosmochimica
466   Acta 105, 316-325.
467   Jørgensen, B., Kasten, S., 2006. Marine geochemistry. Bacteria and.
468   Knipping, J.L., Bilenker, L.D., Simon, A.C., Reich, M., Barra, F., Deditius, A.P., Wälle, M.,
469   Heinrich, C.A., Holtz, F., Munizaga, R., 2015. Trace elements in magnetite from massive iron
470   oxide-apatite deposits indicate a combined formation by igneous and magmatic-hydrothermal
471   processes. Geochimica et Cosmochimica Acta 171, 15-38.
472   Kostka, J.E., Nealson, K.H., 1995. Dissolution and reduction of magnetite by bacteria.
473   Environmental Science & Technology 29, 2535-2540.
474   Larese-Casanova, P., Scherer, M.M., 2007. Fe (II) sorption on hematite: New insights based on
475   spectroscopic measurements. Environmental science & technology 41, 471-477.
476   Li, X., Liu, T., Li, F., Zhang, W., Zhou, S., Li, Y., 2012. Reduction of structural Fe (III) in
477   oxyhydroxides by Shewanella decolorationis S12 and characterization of the surface properties
478   of iron minerals. Journal of soils and sediments 12, 217-227.
479   Lovley, D.R., 1991. Dissimilatory Fe (III) and Mn (IV) reduction. Microbiological reviews 55, 259-
480   287.
481   Lovley, D.R., Phillips, E.J., 1986. Organic matter mineralization with reduction of ferric iron in
482   anaerobic sediments. Applied and environmental microbiology 51, 683-689.
483   Manteca, J.I., García, J.Á.L., Oyarzun, R., Carmona, C., 2014. The beach placer iron deposit of
484   Portman Bay, Murcia, SE Spain: the result of 33 years of tailings disposal (1957–1990) to the
485   Mediterranean seaside. Mineralium Deposita 49, 777-783.
486   Martin, J.H., Fitzwater, S.E., Gordon, R.M., 1990. Iron deficiency limits phytoplankton growth in
487   Antarctic waters. Global Biogeochemical Cycles 4, 5-12.
488   Mazzetti, L., Thistlethwaite, P., 2002. Raman spectra and thermal transformations of
489   ferrihydrite and schwertmannite. Journal of Raman Spectroscopy 33, 104-111.
490   Medina, M., Andrade, S., Faugeron, S., Lagos, N., Mella, D., Correa, J., 2005. Biodiversity of
491   rocky intertidal benthic communities associated with copper mine tailing discharges in
492   northern Chile. Marine Pollution Bulletin 50, 396-409.
493   Morel, F., Price, N., 2003. The biogeochemical cycles of trace metals in the oceans. Science
494   300, 944-947.
495   Morello, E.B., Haywood, M.D., Brewer, D.T., Apte, S.C., Asmund, G., Kwong, Y.J., Dennis, D.,
496   2016. The ecological impacts of submarine tailings placement, Oceanography and Marine
497   Biology. CRC Press, pp. 323-374.
498   Nadoll, P., Angerer, T., Mauk, J.L., French, D., Walshe, J., 2014. The chemistry of hydrothermal
499   magnetite: A review. Ore geology reviews 61, 1-32.
500   Nation, J.L., 1983. A new method using hexamethyldisilazane for preparation of soft insect
501   tissues for scanning electron microscopy. Stain technology 58, 347-351.
502   O'Loughlin, E.J., Gorski, C.A., Scherer, M.M., Boyanov, M.I., Kemner, K.M., 2010. Effects of
503   oxyanions, natural organic matter, and bacterial cell numbers on the bioreduction of

504 lepidocrocite (γ-FeOOH) and the formation of secondary mineralization products.
505 Environmental Science & Technology 44, 4570-4576.
506 Pirbadian, S., Barchinger, S.E., Leung, K.M., Byun, H.S., Jangir, Y., Bouhenni, R.A., Reed, S.B.,
507 Romine, M.F., Saffarini, D.A., Shi, L., 2014. Shewanella oneidensis MR-1 nanowires are outer
508 membrane and periplasmic extensions of the extracellular electron transport components.
509 Proceedings of the National Academy of Sciences 111, 12883-12888.
510 Raiswell, R., Canfield, D.E., 2012. The iron biogeochemical cycle past and present. Geochemical
511 perspectives 1, 1-2.
512 Rajput, S., Pittman Jr, C.U., Mohan, D., 2016. Magnetic magnetite (Fe3O4) nanoparticle
513 synthesis and applications for lead (Pb2+) and chromium (Cr6+) removal from water. Journal of
514 colloid and interface science 468, 334-346.
515 Ramirez-Llodra, E., Trannum, H.C., Evenset, A., Levin, L.A., Andersson, M., Finne, T.E., Hilario,
516 A., Flem, B., Christensen, G., Schaanning, M., 2015. Submarine and deep-sea mine tailing
517 placements: a review of current practices, environmental issues, natural analogs and
518 knowledge gaps in Norway and internationally. Marine Pollution Bulletin 97, 13-35.
519 Roden, E.E., Urrutia, M.M., Mann, C.J., 2000. Bacterial reductive dissolution of crystalline Fe
520 (III) oxide in continuous-flow column reactors. Applied and environmental microbiology 66,
521 1062-1065.
522 Roh, Y., Gao, H., Vali, H., Kennedy, D.W., Yang, Z.K., Gao, W., Dohnalkova, A.C., Stapleton, R.D.,
523 Moon, J.-W., Phelps, T.J., 2006. Metal reduction and iron biomineralization by a
524 psychrotolerant Fe (III)-reducing bacterium, Shewanella sp. strain PV-4. Applied and
525 Environmental Microbiology 72, 3236-3244.
526 Rosselló-Mora, R., Thamdrup, B., Schäfer, H., Weller, R., Amann, R., 1999. The response of the
527 microbial community of marine sediments to organic carbon input under anaerobic conditions.
528 Systematic and Applied Microbiology 22, 237-248.
529 Scott, J.H., Nealson, K.H., 1994. A biochemical study of the intermediary carbon metabolism of
530 Shewanella putrefaciens. Journal of Bacteriology 176, 3408-3411.
531 Shannon, R.D., 1976. Revised effective ionic radii and systematic studies of interatomic
532 distances in halides and chalcogenides. Acta crystallographica section A: crystal physics,
533 diffraction, theoretical and general crystallography 32, 751-767.
534 Shi, L., Dong, H., Reguera, G., Beyenal, H., Lu, A., Liu, J., Yu, H.-Q., Fredrickson, J.K., 2016.
535 Extracellular electron transfer mechanisms between microorganisms and minerals. Nature
536 Reviews Microbiology 14, 651.
537 Stucki, J., 1981. The quantitative assay of minerals for Fe2+ and Fe3+ using 1, 10-
538 phenanthroline: II. A photochemical method 1. Soil Science Society of America Journal 45, 638-
539 641.
540 Tang, Y.J., Meadows, A.L., Kirby, J., Keasling, J.D., 2007. Anaerobic central metabolic pathways
541 in Shewanella oneidensis MR-1 reinterpreted in the light of isotopic metabolite labeling.
542 Journal of Bacteriology 189, 894-901.
543 Thamdrup, B., 2000. Bacterial manganese and iron reduction in aquatic sediments, Advances in
544 microbial ecology. Springer, pp. 41-84.
545 Tronc, E., Belleville, P., Jolivet, J.P., Livage, J., 1992. Transformation of ferric hydroxide into
546 spinel by iron (II) adsorption. Langmuir 8, 313-319.
547 Tugel, J.B., Hines, M.E., Jones, G.E., 1986. Microbial iron reduction by enrichment cultures
548 isolated from estuarine sediments. Applied and environmental microbiology 52, 1167-1172.
549 Williams, A.G., Scherer, M.M., 2004. Spectroscopic evidence for Fe (II)– Fe (III) electron
550 transfer at the iron oxide– water interface. Environmental science & technology 38, 4782-
551 4790.
552 Young, R., 1995. The Rietveld Method, International Union of Crystallography Monographs on
553 Crystal and Oxford Science Publications. Oxford, UK.

554   Zachara, J.M., Fredrickson, J.K., Smith, S.C., Gassman, P.L., 2001. Solubilization of Fe (III) oxide-
555   bound trace metals by a dissimilatory Fe (III) reducing bacterium. Geochimica et Cosmochimica
556   Acta 65, 75-93.

557

Figure Captions

Figure 1. Variation in concentration of lactate, acetate and total aqueous Fe over time in the bioreductive dissolution experiments with synthetic and commercial iron oxide samples: a. Hematite , b. Goethite , c. Magnetite , d. Ferryhydrite . Key: (□) Lactate; (▲) Acetate; (●) Total dissolved iron and (o) Abiotic controls. Error bars correspond to the analytical uncertainty (SD).

Figure 2. Variation in concentration of lactate, acetate and total aqueous Fe over time in the bioreductive dissolution experiments with field powdered samples. a. Sample V1 (Distrito Algarrobo, Chile); b. Sample M1 (Malmberget, Sweden); c. Sample TB (Lago Sur, Chile). Key: (□) Lactate; (▲) Acetate; (●) Total dissolved iron and (o) Abiotic controls. Error bars correspond to the analytical uncertainty (SD).

Figure 3. Iron bioreduction coefficients of the iron oxides mediated by *S. loihica*: a) values normalized to mass and b) normalized to surface area.

Figure 4. Ferrous iron adsorption isotherm onto ferrihydrite in the marine medium. Dashed line indicates the saturation point based on the calculated number of sorption sites for ferrihydrite. Dotted lines indicate the SD of the experiment.

Figure 5. XRD patterns of non-reacted pure ferrihydrite (red) and reacted ferrihydrite after absorption experiments (black). Blue lines indicate the position of the main XRD peaks of pure crystalline magnetite (blue) obtained from Ruff database. Most of the reacted ferrihydrite transformed to magnetite after surface adsorption of iron (II). Rietveld analysis of the reacted sample indicates that 10 % of the sample is ferrihydrite and 90% is magnetite with nanocrystalline morphology.

Figure 6. SEM images of *S. loihica* cells colonizing an iron-oxide surface: a) Bacteria growing preferably on the oxide surfaces (magnetite); b,c) Bacteria growing on the surface of magnetite (M1) with developed extracellular structures (see arrows) interconnecting cells and/or connecting cells with the mineral surface.

584　7　Table heads

585　**Table 1.** Surface area and mineralogical composition (wt. %) of the studied samples.

586　**Table 2.** Microbial bioreduction activity coefficients calculated from measured acetate
587　and ferrous iron concentrations.

588